Cement & Concrete Composites 40 (2013) 14–20

Contents lists available at SciVerse ScienceDirect

Cement & Concrete Composites

journal homepage: www.elsevier.com/locate/cemconcomp

Incorporating carbon sequestration materials in civil infrastructure: A micro and nano-structural analysis

Paulo J.M. Monteiro [a,*], Laurence Clodic [b], Francesco Battocchio [c], Waruntorn Kanitpanyacharoen [d], Sejung Rosie Chae [a], Juyoung Ha [e], Hans-Rudolf Wenk [d]

[a] Department of Civil Engineering, University of California, Berkeley, CA 94720, United States
[b] Calera Corporation, Los Gatos, CA 95032, United States
[c] Department of Engineering, Cambridge University, Cambridge, UK
[d] Department of Earth and Planetary Science, University of California, Berkeley, CA 94720, United States
[e] School of Environmental and Life Sciences, Kean University, Union, NJ 07083, United States

ARTICLE INFO

Article history:
Received 22 November 2011
Received in revised form 17 March 2013
Accepted 21 March 2013
Available online 2 April 2013

Keywords:
Calcium carbonate
Carbon sequestration
Cement
Concrete
Microstructure

ABSTRACT

The Calera method for carbon sequestration promotes carbon mineralization through aqueous precipitation. This work reports a comprehensive analysis on a carbonate obtained by the Calera process to evaluate its suitability as a cement replacement for concrete applications. This work focuses on the analysis of two hydrated cement pastes made with a blend of Portland cement and Calera carbonates by various advanced analytical techniques. Scanning Electron Microscopy (SEM) equipped with Energy Dispersive Spectroscopy (EDS) was used to observe microstructures and determine elemental compositions. The synchrotron X-ray diffraction technique combined with Rietveld analysis were applied to identify constituent phases and refine crystal structures, crystallite sizes as well as relative phase abundances. Calcite and vaterite are observed in all samples while CSH II and portlandite are dominant in the cement pastes. Near-Edge X-ray Absorption Fine Structure (NEXAFS) spectrometry and Scanning Transmission X-ray Microscopy (STXM) experiments were conducted to investigate chemical speciation and morphological information of carbonate minerals with different absorption energies. STXM results confirmed heterogeneity of the samples, and also provided a nano-scale phase map across multiple particles. Differential Thermogravimetric (DTG) was used to observe heat transfer through structures and changes in mass upon heating. A compressive strength tests were performed on materials and shown comparable strength to Portland cement.

1. Introduction

Concrete is the most widely used construction material, consuming 2.6 billion tonnes per year of Portland cement [1], and producing CO_2 1.88 billion tonnes per year [2]. Substantial consumption of concrete for infrastructure makes it uniquely qualified for being a host for carbon sequestration storage. Although, this seems to be an attractive solution in reducing CO_2 emissions, regulatory approval requires a general understanding of the effects of incorporating sequestered materials and the ability to make accurate estimates for specific applications is necessary. Currently, the following possibilities exist: (1) capturing carbon and then converting it to solid carbonates for use in concrete [3] and (2) impressing critical carbon gas into fresh concrete to create industrial products [4].

Calera Corporation has developed an innovative method for carbon sequestration through Carbonate Mineralization by Aqueous Precipitation (CMAP) method [3]. The fundamental of CMAP process is to capture raw flue gas emission such as CO_2 from a gas- or coal-fired power plant, convert into carbonates, and eventually react with binding species such as calcium or magnesium. The output materials are further dissolved in a high pH aqueous solution and combined with different divalent cations to precipitate carbonate minerals. These Ca- and Mg-containing carbonate minerals are stable and usable as supplementary cementitious materials or as aggregates for concrete.

It is thus essential to evaluate physical and chemical properties of Calera carbonates to ensure that they meet the Portland cement standards. The first goal of this work is to characterize the composition and morphology of a carbonate precipitate (PRECIPITATE I), which exhibits a good compressive strength performance when blended with Portland cement. A second goal of the experiment is to determine the effect of the calcium carbonate minerals such as calcite and vaterite on the early stages of cement hydration in

* Corresponding author. Tel.: +1 510 643 8251; fax: +1 510 643 5264.
E-mail address: monteiro@ce.berkeley.edu (P.J.M. Monteiro).

0958-9465/$ - see front matter © 2013 Elsevier Ltd. All rights reserved.
http://dx.doi.org/10.1016/j.cemconcomp.2013.03.013

two different cement pastes (PASTE A and PASTE B). By combining data obtained from various advanced analytical techniques, accurate identification and comprehensive evaluation of Calera materials can be accomplished.

2. Materials and methods

2.1. Materials

The Calera PRECIPITATE I was produced by adding caustic solution to a brine made of seawater and $CaCl_2$, and circulating CO_2 throughout this brine to produce a carbonate precipitate. The precipitated material was rinsed in a slurry form and then spray-dried.

Two additional Calera precipitates (PRECIPITATE II and PRECIPITATE III) were synthesized to determine the effect of calcium carbonate on the early hydration stages of ordinary Portland cement (OPC). These two carbonate precipitates were used as cementitious minerals to further produce cement pastes. Samples PRECIPITATE II and PRECIPITATE III were prepared in an identical process, but PRECIPITATE III was prepared in a small 4-l batch whereas PRECIPITATE II was prepared in a larger 96-gallon batch. A small amount of halite (NaCl) was observed after the rinsing step, indicating the rinsing process was not done as thoroughly as for PRECIPITATE III.

Two cement paste samples (PASTE A and PASTE B) were prepared at a liquid-to-powder ratio of 0.80, using approximately 10 g of Calera carbonate precipitate (PRECIPITATE II and PRECIPITATE III, respectively) and 40 g type II/V of OPC. The mixtures were cured at 23 °C in sealed containers for 7 days. Both cement pastes were ground after 7 days with acetone treatment and dried for 24 h in a desiccator at room temperature.

All samples were first analyzed with an SEM for microstructures and elemental composition and then measured with synchrotron X-ray diffraction to identify constituent phases and quantify relative phase abundance as well as crystallite sizes. Near-Edge X-ray Absorption Fine Structure spectrometry and Scanning Transmission X-ray Microscopy (NEXAFS–STXM) techniques were applied to verify the chemical speciation.

2.2. Scanning Electron Microscope (SEM)

A small amount of PRECIPITATE I, PASTE A and PASTE B was placed on carbon tapes and examined with a Hitachi FE-SEM SU6600. To obtain good resolution images, the SEM was operated under a variable pressure mode with an accelerating voltage of 15 kV and a probe current of 42,000 nA. Backscattered (BE) SEM images shows homogeneous microstructures of calcium carbonates in the samples (Fig. 1A and B). Compositional maps of Si, Ca, Mg and C were collected with an Oxford Instrument equipped with the INCAx-act energy dispersive X-ray spectroscopy Silicon Drift Detector (SDD) system.

2.3. Synchrotron X-ray diffraction

The synchrotron X-ray diffraction measurements were done on PRECIPITATE I, PASTE A and PASTE B at beamline BESSRC 11-ID-C of the Advanced Photon Source (APS) of Argonne National Laboratory. The samples were ground into fine-grained powder and stored inside 1.5 mm-diameter kapton tubes. The X-ray beam with a wavelength of 0.1079 Å was used to penetrate through the samples and produce diffraction images, which were collected on a Mar345 image plate detector (3450 × 3450 pixels) positioned approximately 2 m from the sample. Each sample was exposed for 50 s and recorded within a 2θ range from 0° to 7.5°.

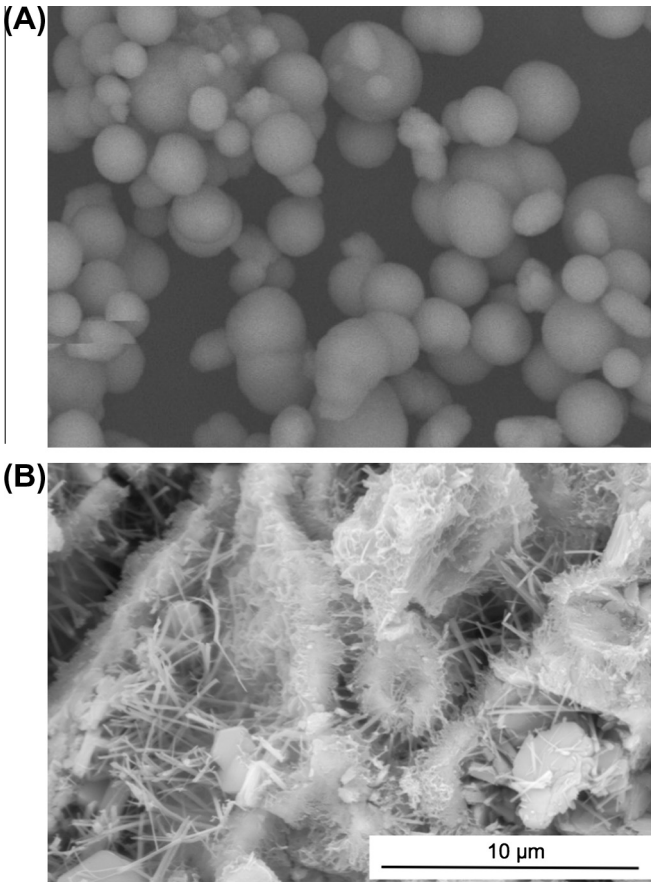

Fig. 1. Backscattered-SEM images of (A) PRECIPITATE I and (B) PASTE B.

The instrument geometry (e.g., sample-to-detector distance, X-ray beam center, and tilt angles) was calibrated with a CeO_2 standard. The spectra of diffraction images are expressed as a function of $Q = 2\pi/d$ rather than d-spacing (Q = 0–3.5 $Å^{-1}$) (Fig. 2A–C). The Rietveld method [5] implemented in the Materials Analysis Using Diffraction (MAUD) software [6] was used to refine crystal structures, microstructural parameters, and volume fractions. More details about the experimental setup and Rietveld analysis can be found in Wenk et al. [7]. Starting crystal structures of different phases were used as following: calcite [8], vaterite [9], portlandite [10], ettringite [11], brownmillerite [12], monocarboaluminate [13], C_2S [14], C_3S [15], CSH I refined from tobermerite [16], and CSH II refined from jennite [15].

2.4. Scanning Transmission X-ray Microscopy (STXM)

The synchrotron STXM measurements were conducted at beamline 5.3.2.2 of the Advanced Light Source (ALS) at Lawrence Berkeley National Laboratory. Powder samples of PRECIPITATE I and PASTES A and PASTE B were embedded in a Petroplexy epoxy under vacuum and followed by microtoming at 0.15 μm thickness. The image contrast was obtained from differential absorption of X-ray, depending on the chemical composition of the sample (Fig. 3). STXM data were collected by scanning the sample in the x–y direction (image stack) or x direction (line scan) of selected sample areas at energy increments of 0.1–0.25 eV over the energy range of interest (e.g., 280–305 eV for carbon and 342–360 eV for calcium) (Fig. 3). The stack images not only provide two-dimensional resolution, but also produce a NEXAFS spectrum for a specific element on each pixel of the image. The best attainable spatial resolution is 25 nm. Counting times for the images were typically

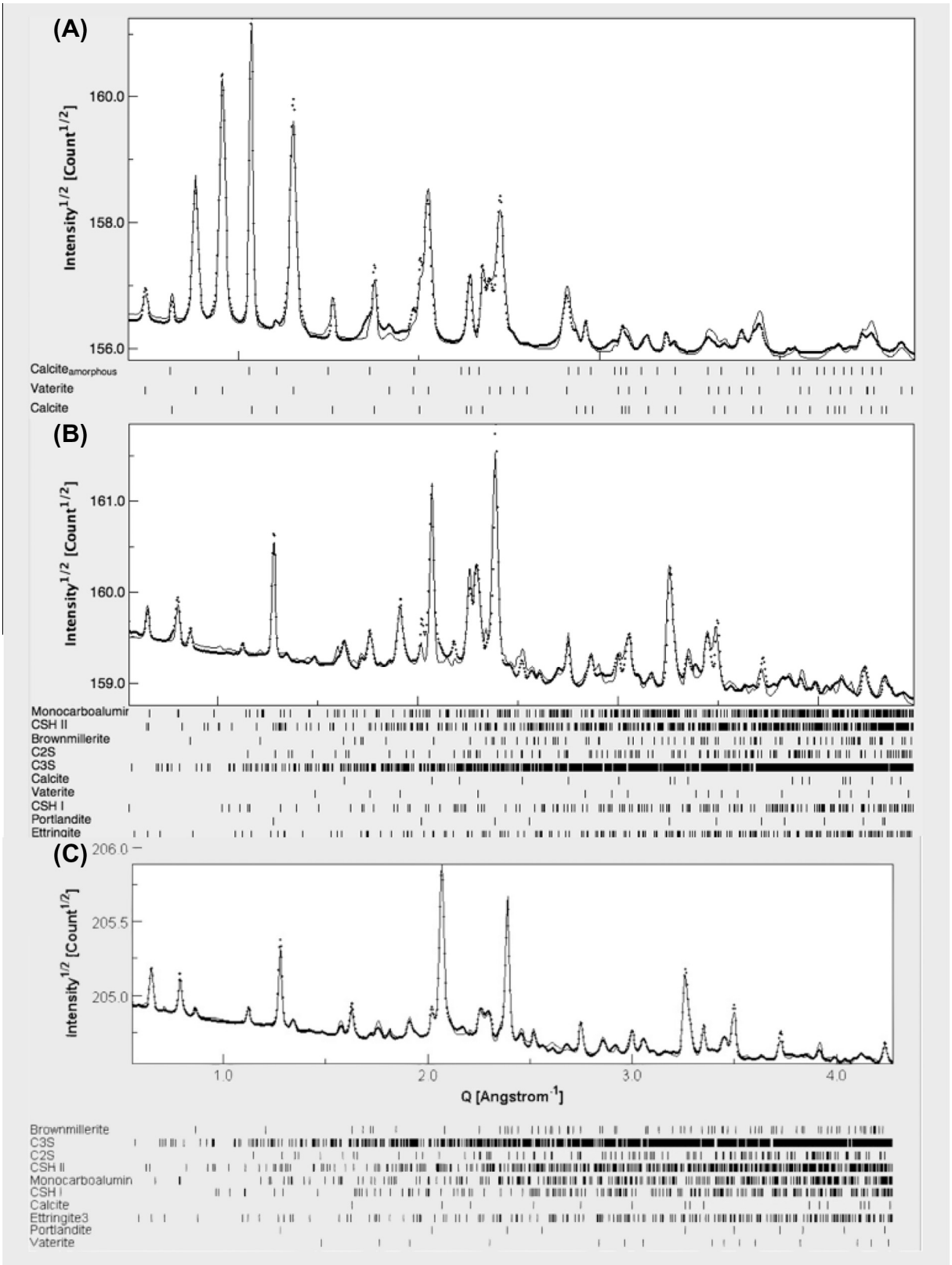

Fig. 2. Synchrotron diffraction spectra of (A) PRECIPITATE I, (B) PASTE A, and (C) PASTE B. The calculated model (thin black solid) are compared with the experimental data (thick black solid), indicating excellent fits both peak positions and intensities.

less than 2 ms per pixel to avoid beam damage. Energy calibration was accomplished using the well-resolved 3p Rydberg peak of gaseous CO_2 for the C K-edge and calcite for the Ca $L_{II,III}$-edge. Normalization and background subtraction of the spectra were performed by dividing each spectrum from the sample by the spectrum of the sample-free location. Elemental maps of the samples were obtained by subtracting the image obtained from the below the absorption energy level and the image obtained above the

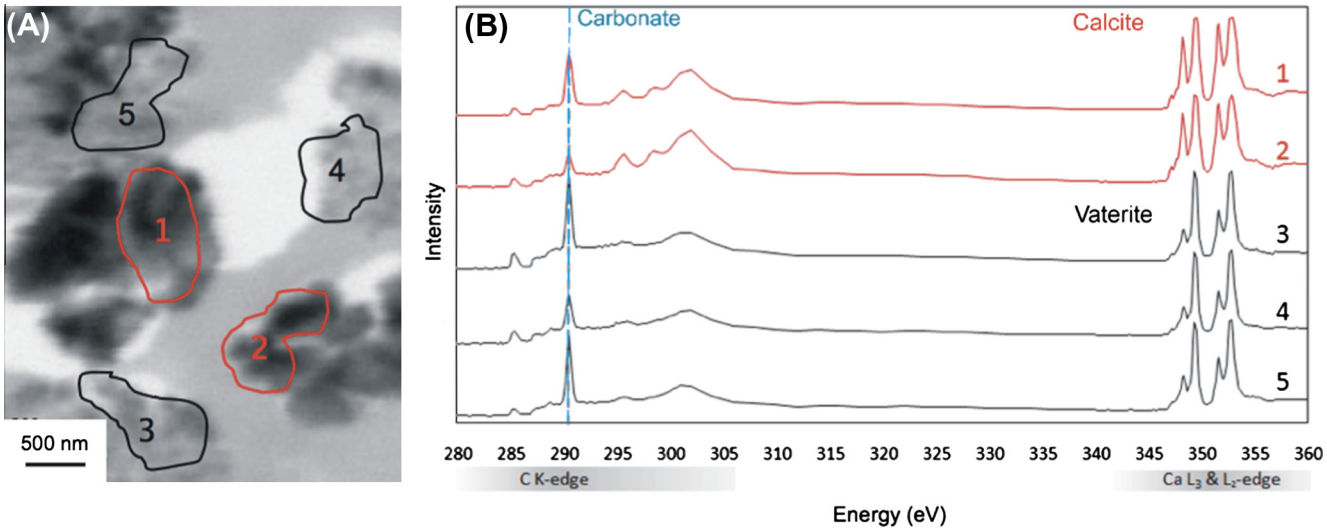

Fig. 3. (A) STXM image of selected areas of PRECIPITATE I taken at Ca $L_{II,III}$-edge for NEXAFS analysis. (B) NEXAFS spectra at C K-edge and at Ca $L_{II,III}$-edge.

absorption energy. Beam damage on the samples was checked by comparing the NEXAFS spectra of the samples at the same position after taking all the STXM measurements. No noticeable changes in NEXAFS spectra were observed in any of the samples, suggesting no significant damage from the beam had occurred. Axis 2000 software (August 2009 version) was used to align image stacks and extracted NEXAFS spectra from image stack or line scan measurements.

2.5. Differential Thermogravimetry (DTG)

Thermogravimetry measures the changes of weight in a sample under different conditions. The measurement can be done on samples that are heated, cooled or maintained at a constant temperature. For PRECIPITATE I, the amount of non-evaporable water and CO_2 is determined as the weight loss until 600 °C and between 600 °C and 900 °C. The amount of hydrate bound water and $Ca(OH)_2$ for PASTES A and B is determined between 60 °C and 400 °C, and 400 °C and 500 °C, respectively. The amount of CO_2 bound either in carboaluminate phases ($CaO–Al_2O_3–CO_2–H_2O$ system) or in $CaCO_3$ phases is calculated from the weight loss between 500 °C and 900 °C.

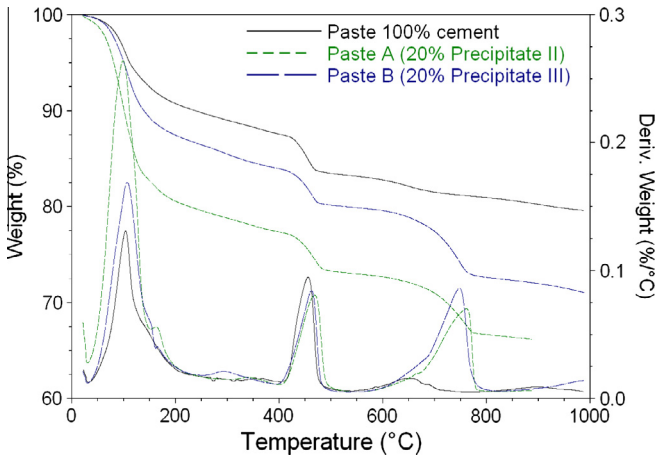

Fig. 4. A comparison of TGA analysis between (A) a neat Portland cement paste (blue) and (B) a mixture of Portland cement paste (80%) blended with PRECIPITATE III (20%) (green). Both pastes were cured for 7 days. (For interpretation of the references to color in this figure legend, the reader is referred to the web version of this article.)

Simultaneous Thermal Analysis (STA), which includes simultaneous data collection of Differential Scanning Calorimetry (DSC) and Thermogravimetry Analysis (TGA), were done by TA Instrument model Q600 SDT. DSC and TGA data were measured under identical conditions (Fig. 4). Approximately 30 mg of ground PRECIPITATE II and III were poured in Al_2O_3 crucible and treated from ambient temperature to 1000 °C, using N_2 purge gas with an injection rate of 50 ml per minute and with a heating rate of 20 °C per minute.

3. Results

3.1. PRECIPITATE I

The PRECIPITATE I sample is composed of spherical aggregates of fibrous crystallites, mostly less than 3 μm in size and often clustered together (Fig. 1A). The ellipsoids of calcite crystallites, approximately 2 μm in size, are also displayed in the same figure. Rietveld refinement of synchrotron X-ray (Fig. 2A) spectra identified three constituent minerals: vaterite, calcite, and an amorphous carbonate phase. Vaterite is most abundant (73 wt.%) while the amorphous phase is the least (3 vol.%). The amorphous phase was used to fit diffuse peaks observed at $Q = 2.7$ Å^{-1} and 4.1 Å^{-1}. The addition of this phase improves quantitative analysis. Fig. 2A compares the calculated model and experimental spectra, which indicates an excellent fit. The volume fraction for each phase are shown in Table 1.

A STXM image and NEXAFS spectra of Ca $L_{II,III}$-edge and C K edge of PRECIPITATE I are illustrated in Fig. 3. There are noticeable differences between measured spectra, suggesting heterogeneity in the sample. The NEXAFS spectra of Ca $L_{II,III}$-edge collected from area 1 and 2 have peak intensity and peak position similar to calcite, whereas spectra taken from areas 3, 4, and 5 correspond to vaterite, based on previously collected mineral standards [17].

3.2. Cement PASTE A

Cement PASTE A is composed of 20% carbonate PRECIPITATE II and mostly fine-grained crystals less than 10 μm. Rietveld analysis of spectra indicate a composition of at least ten minerals in the sample (Fig. 2B and Table 1). CSH I (24 vol.%) and portlandite

Table 1
A summary of quantitative phase volume fractions of PRECIPITATE I, PASTE A and PASTE B obtained from synchrotron X-ray diffraction data.

Phases	Volume%		
	PRECIPITATE I	PASTE A	PASTE B
Vaterite	72.21(8)	17.50(4)	5.38(9)
Calcite	21.58(7)	14.02(7)	13.60(1)
Calcite amorphous	6.20(2)	–	–
Portlandite	–	16.58(5)	13.39(1)
Ettringite	–	1.63(9)	11.18(1)
Monocarboaluminate	–	11.11(6)	8.21(1)
Brownmillerite	–	6.82(6)	2.90(5)
C_2S	–	8.90(6)	2.92(6)
C_3S	–	5.78(5)	1.70(4)
CSH I	–	13.35(6)	3.04(4)
CSH II	–	4.30(1)	37.59(4)

(22 vol.%) are the dominant phases. The calculated peak profile (solid line) is compared with experimental data (dotted line), indicating again close similarity indicative of an excellent fit, both in intensities as well as position of diffraction peaks.

3.3. Cement PASTE B

The microstructure and surface topology of PASTE B (Fig. 1B), which contains 20% of PRECIPITATE III, is similar to that of PASTE A. PASTE B (Fig. 2C, Table 1) is also composed of the same ten minerals that were observed in cement PASTE A, but here the most abundant phases are CSH II (37 vol.%), calcite (13 vol.%), portlandite (13 vol.%) and ettringite (11 vol.%).

DTG analysis of PASTE A and PASTE B was compared to a pure Portland cement paste (blue line in Fig. 4). The observation of water loss below 400 °C indicates an acceleration of the cement hydration for the blended paste compared to the neat paste. This is a common effect observed for finely divided calcium carbonates as they provide additional nucleation surfaces for hydration of Portland cement to occur. Despite the 20% dilution factor, the amount of portlandite formed remains similar (as shown by the DTG peaks centered around 450 °C), which further supports the concept of an acceleration of the cement hydration for the blended Calera cement paste compared to the pure Portland cement paste.

4. Discussion

One of the goals of this study was to investigate the interaction of vaterite with the Portland cement phases. Most of the published literature regarding the reactivity of calcium carbonates blended with Portland cement has been obtained using pure calcite or ground limestone [18,19]. Calcite in these forms is usually considered as a filler in Portland cement hydration, participating only to a limited extent (1–5% depending on the cement Al_2O_3 content) in the hydration reactions by forming analogs of calcium aluminosulfate hydrates (typically present in Portland cement pastes), in which the sulfates are replaced by carbonates: monocarboaluminate and hemicarboaluminate [20]. The formation of carboaluminates prevents the transition of ettringite to monosulfoaluminate usually observed in carbonate-free pastes. To a lesser extent, carbonates are also shown to enter in the composition of calcium silicate hydrates and lower the portlandite content.

In this study, the Calera precipitates were shown to be composed of calcium carbonate polymorphs: calcite, vaterite, and an amorphous magnesium–calcium carbonate phase. The results obtained on the pastes aged for 7 days indicate that vaterite, despite its metastable character, remains stable in the paste and reacts to a limited extent along with calcite to form monocarboaluminate. This is illustrated in Fig. 5 on the EDS maps of 7-day paste fracture surfaces which still display clear evidence of spherical vaterite particles.

Another interesting aspect of this study is to assess how the carbonate polymorphs present in the precipitate interact with the cement phases. Synchrotron X-ray diffraction (Fig. 2) and TGA results (Fig. 4) obtained for paste specimens, at which the hydration was halted at different ages, ranging from a few minutes to 28 days, indicate that the presence of the precipitate does not alter the initial hydration reactions of the Portland cement with similar sequence of formation of hydrates (portlandite, ettringite, etc.), whether or not the precipitate is present. The main difference is noted in the stabilization of ettringite by the formation of monocarboaluminate hydrate as shown by Matschei et al. [20] for Portland cement – limestone systems. Thermogravimetric analysis results indicate an acceleration of the reactions as shown by the similar amounts of portlandite (DTG peak around 450 °C) and increased amounts of other hydrates (TGA loss up to 250 °C), which is also reflected in higher compressive strengths at early age.

The compressive strengths of cubes were measured according to the ASTM C109 standard test method up to 28 days (Fig. 6). Results indicate that the presence of Calera carbonates is beneficial for compressive strength at early age (1 and 7 days) as it shows higher strengths than mixtures that do not contain Calera carbonates. By 28 days, the compressive strengths obtained for the plain OPC mixtures are slightly higher.

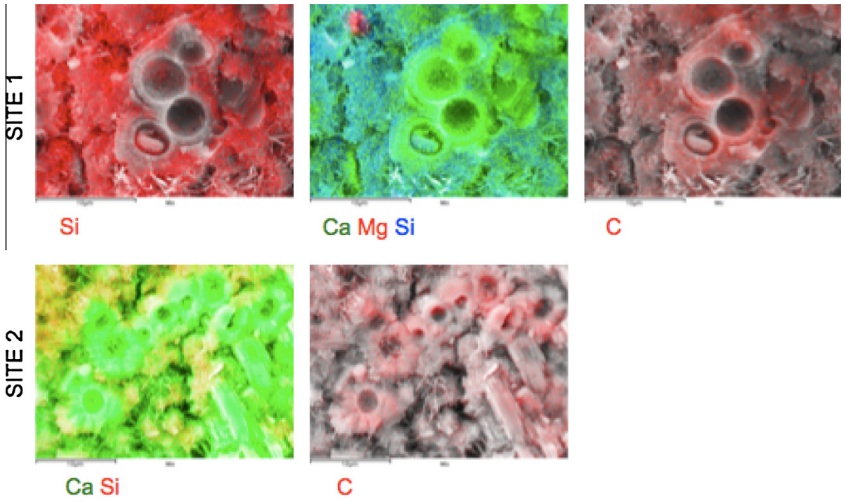

Fig. 5. EDS analysis of PASTE B showing elemental distributions of C, Ca, Si, and Mg in two different areas (SITE 1 and SITE 2).

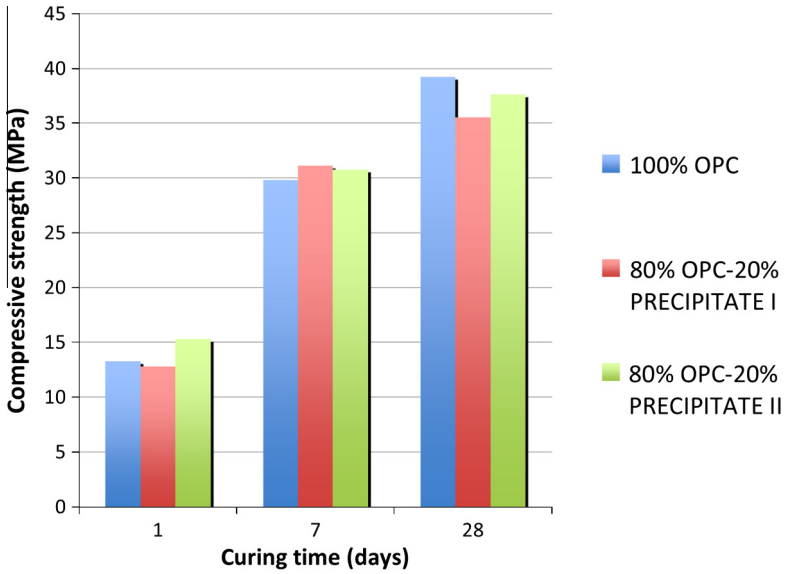

Fig. 6. A comparison of compressive strength evolution of cement pastes made with (a) 100% ordinary Portland cement (OPC) (blue) (b) 80% OPC and 20% PRECIPITATE I (red) and (c) 80% OPC and 20% PRECIPITATE II (green). (For interpretation of the references to color in this figure legend, the reader is referred to the web version of this article.)

SEM, which produces high-resolution images of sample topology and microstructural characteristics, can capture images of large area and bulk volume of sample in details. In particular, Fig. 1A displays spheres of vaterite and ellipsoids of calcite while Fig. 1B illustrates needle-shape crystals of ettringite and platelets of phases that could be identified as monocarboaluminate and/or portlandite are shown as growing on the surface of the precipitate vaterite spheres in PASTE B. In addition, the SEM-EDS system can be used to illustrate the distribution of different elements in a sample (Fig. 5). These combined techniques successfully measure the elemental abundance, determine its preliminary composition, and sufficiently observe surface topography. The identification of mineral phases in each sample is based on the elemental composition found with the SEM and the diffraction pattern refined with the Rietveld method. The method shows an amazing resolution to characterize components of multiphase materials with overlapping peaks.

Results from STXM further confirmed the heterogeneity of the samples, especially in Ca-containing mineral phases. It should be noted that all the C K-edge NEXAFS spectra from the samples contained strong peaks at 290.3 eV, which correspond to carbonate peaks. STXM effectively provides information on the coordination environments for different elements and reveals information on spatial heterogeneity. In addition, the cluster of pure phases observed in STXM analysis complement morphological observation from the SEM analysis. Although it is difficult to distinguish spheres from ellipsoids from a microtomed sample, an apparent lack of inter particle heterogeneity agrees wit SEM observation.

5. Conclusion

The use of SEM imaging along with EDS chemical analysis provide useful information to understand surface topography and microstructures, to determine preliminary elemental characterization, and to quantify the composition. The synchrotron X-ray diffraction technique combined with the Rietveld analysis was employed to identify the mineral phases and successfully quantify phase fractions in each sample. Results from STXM provided further information on different chemical speciation and coordination environments. The DTG analysis of two cement pastes confirms the formation of a carboaluminate phase and its effect on ettringite stabilization (i.e., absence of transformation to monosulfoaluminate hydrate). It is revealed that vaterite remains stable inside a Portland cement paste under alkaline conditions even though it is metastable compared to calcite. In addition, DTG analysis correlates well with the favorable strength development at early age, the strength of neat Portland mortars, and the increased hydration reactivity for the vaterite-containing paste. In summary, the experimental results indicate that the studied carbon sequestration materials interact well with the hydration products of Portland cement and have the potential of being used in concrete. Cast-in-place and manufactured concrete demonstration projects requiring reduced carbon footprints were successfully delivered in Northern California on the basis of these beneficial properties.

Acknowledgments

The authors would like to thank the financial support given by Calera Co. to study carbon sequestration materials. We are appreciative an access to beamline BESSRC 11-ID-C at the Advanced Photon Source (APS), which is supported by the U.S. DOE, Argonne National Laboratory under Contract No. DE-AC02-06CH11357, and Dr. David Kilcoyne at beamline 5.3.2 at the Advanced Light Source (ALS), which is supported by the Director, Office of Science, Office of Basic Energy Sciences, of the U.S. Department of Energy under Contract No. DE-AC02-05CH11231.

References

[1] Oss HGV. U.S. Geological Survey Mineral Commodity Summaries: cement. In: USGS; 2011. p. 2.
[2] Taylor M, Tam C, Gielen D. Energy efficiency and CO_2 emissions from the Global Cement Industry. In: IEA-WBCSD workshop: energy efficiency and CO_2 emission reduction potentials and policies in the Cement Industry, Paris, France; 2006.
[3] Constantz BR, Cecily R, Clodic L. Hydraulic cements comprising carbonate compound compositions. In: Corporation C, editor, USA; 2009.
[4] Fernández Bertos M, Simons SJR, Hills CD, Carey PJ. A review of accelerated carbonation technology in the treatment of cement-based materials and sequestration of CO_2. J Hazard Mater 2004;B112:193–205.
[5] Rietveld HM. A profile refinement method for nuclear and magnetic structures. J Appl Crystallogr 1969:65–71.
[6] Lutterrotti L, Matthies S, Wenk H-R, Shchultz AJ, Richardson JW. Combined texture and structure analysis of deformed limestone from time-of-flight neutron diffraction spectra. J Appl Phys 1997;81:594–600.

[7] Wenk H-R, Voltolini M, Mazurek M, Loon LRV, Vinsot A. Preferred orientations and anisotropy in shales: Callovo-Oxfordian shale (France) and Opalinus clay (Switzerland). Clays Clay Miner 2008;56:285–306.
[8] Maslen EN, Streltsov VA, Streltsova NR. X-ray study of the electron density in calcite, $CaCo_3$. Acta Crystallogr Sec B 1993;49:636–64.
[9] Kamhi SR. On the structure of vaterite, $CaCO_3$ locality: synthetic. Acta Crystallogr 1963;16:770–2.
[10] Nagai T, Ito T, Hattori T, Yamanaka T. Compression mechanism and amorphization of portlandite, $Ca(OH)_2$: structural refinement under pressure sample: $P = 0.5$ GPa. Phys Chem Miner 2000;27:462–6.
[11] Moore AE, Taylor HFW. Crystal structure of ettringite locality: Scawt Hill, Northern Ireland. Acta Crystallogr 1970;B26:386–93.
[12] Bertaut EF, Blum P, Sagnieres A. Structure du ferrite bicalcique et de la brownmillerite. Acta Crystallogr 1959;12:149–59.
[13] Francois M, Renaudin G, Evrard OA. Cementitious compound with composition $3CaO{\cdot}Al_2O_3{\cdot}CaCO_3{\cdot}11H_2O$. Acta Crystallogr 1998;C54:1214–7.
[14] Tsurumi T, Hirano Y, Kato H, Kamiya T, Daimon M. Crystal structure and hydration of belite locality: synthetic. Ceram Trans 1994;40:19–25.
[15] Bonaccorsi E, Merlino S, Taylor HFW. The crystal structure of jennite, Ca9Si6O18(OH)6*8H2O locality: Fuka Japan. Cem Concr Res 2004;34:1481–8.
[16] Merlino S, Bonaccorsi E, Armbruster T. The real structure of tobermorite 11A: normal and anomalous forms, OD character and polytypic modifications. Eur J Miner 2001;13:557–90.
[17] Benzerara K, Yoon TH, Tyliszczak T, Constantz B, Spormann AM, Brown Jr GE. Scanning transmission X-ray microscopy study of microbial calcification. Geobiology 2004;2:249–59.
[18] Hawkins P, Tennis P, Detwiler R. The use of limestone in Portland cement: a state-of-the-art review. In: Skokie (Illinois): Portland Cement Association; 2003. p. 44.
[19] Gabrovšek R, Vuk T, Kaucic V. Evaluation of the hydration of Portland cement containing various carbonates by means of thermal analysis. Acta Chim Slov 2006;53:159–65.
[20] Matschei T, Lothenbach B, Glasser FP. The role of calcium carbonate in cement hydration. Cem Concr Res 2007;37:551–8.